

Explosive ionization of molecules in intense laser fields

M. Ivanov, T. Seideman, and P. Corkum

Steacie Institute for Molecular Sciences, National Research Council of Canada, Ottawa, Ontario, Canada K1A 0R6

F. Ilkov

Centre d'Optique, Photonique et Laser, Université de Laval, Québec, Québec, Canada G1K 7P4

P. Dietrich

Institut für Experimentalphysik, Freie Universität Berlin, 14195 Berlin, Germany

(Received 7 November 1995)

We discuss the mechanisms of multielectron dissociative ionization of diatomic molecules in intense laser fields. We show that during dissociation of molecular ions the nuclei pass through a critical range of internuclear distances where ionization is enhanced by several orders of magnitude for *several successive charge states of the molecule*. The critical range of internuclear distances depends only weakly on the laser frequency, laser intensity, and the charge state. Both numerical and analytical models are developed, and the effect of enhanced ionization on the kinetic energy and angular distributions of charged fragments is discussed. [S1050-2947(96)00208-9]

PACS number(s): 33.80.Rv, 82.50.Fv

I. INTRODUCTION

We describe a quantitative model of molecular ionization in intense laser fields. We show that the multiple-well nature of the potential for electron motion in a molecular ion introduces new ionization mechanisms which are not present in an atom. Under certain conditions the ionization potential of a molecule is neither the only nor the most important parameter in determining its ionization dynamics. As a result, systems with high ionization potentials can ionize more efficiently than systems with much lower ionization potentials.

We show that the ionization rate of several successive charge states of a diatomic molecule is highly sensitive to the internuclear separation R and has a pronounced peak in a certain critical region of R . For fixed intensity the peak position is almost independent of the charge state and wavelength. Based on this result, we suggest a scenario of multielectron dissociative ionization of diatomic molecules in intense laser fields. The basic mechanism behind enhanced ionization of molecular ions has very broad implications, ranging from optical breakdown in ultrashort pulses to cluster ionization.

The advent of short pulse lasers capable of producing intensities of 10^{15} – 10^{16} W/cm² about a decade ago raised initial hopes of exciting collective multielectron dynamics in atoms. A series of experiments [1–4] demonstrated that an atom can be stripped of its outer electronic shell at intensities still below 10^{16} W/cm². Motivated by these experiments, a “shell explosion” model [5] suggested that very intense fields excite a collective motion of outer-shell electrons, which then scatter from the parent ion core, resulting in simultaneous ejection of the whole valence shell. However, the smooth nature of a laser pulse presents a serious obstacle for simultaneous multielectron ionization [6]. In all experiments the field passes the region of lower intensities before reaching the high intensities at which collective excitations might occur. Electrons are stripped one by one, at well defined

threshold intensities, and ionization is sequential [6].

The search for simultaneous ionization of many electrons motivated seminal experiments [7] on ionization of diatomic molecules. The idea behind the experiment [7] was simple and elegant: If simultaneous ionization were possible, e.g., for a Xe atom, it would lead to an easily observable effect for an isoelectronic HI diatomic molecule. Shell explosion of HI will produce highly charged molecular ions, e.g., HI^{6+} , at the equilibrium distance of a neutral molecule ($R=1.61$ Å for HI). Further dissociation of the molecular ion due to the Coulomb repulsion of its highly charged nuclei would yield fragments (H^+ and I^{5+}) with total kinetic energy of about 45 eV. The experimentally detected energy was much lower (21 eV). The same was found in a similar experiment for an N_2 molecule [8].

Although disappointing from the point of view of collective processes, the experiments [7,8] revealed a different surprising effect: The highly complex process of multielectron dissociative ionization of molecules yielded a remarkably simple spectrum of the kinetic energies of fragments. Namely, the kinetic energy released in all fragmentation channels gave very well resolved lines, rather than smooth energy distribution.

A qualitative model of multiple dissociative ionization proposed in [9] to explain the experimentally observed line structure in the kinetic energy of the fragments suggested that each charged state of a diatomic molecular ion is produced at its own well defined value of the internuclear separation, which depends on the laser intensity and the charge state. Since in this model the optimum values of R were different for different charge states, the nuclei were expected to travel along the repulsive Coulomb potential surfaces between successive ionization stages. Nonetheless, it was suggested by several experiments and conclusively demonstrated in [10], that the atomic fragments possess kinetic energies which constitute a constant fraction of the Coulomb repulsion experienced by the molecular ion at the equilib-

rium distance. This observation holds for all studied simple molecules, *independent of the charge state, pulse duration, frequency and intensity of the laser pulse* [10]. The “magic” ratio of the measured kinetic energy to the energy of the Coulomb repulsion at the equilibrium distance depends only on the molecule, in contrast with the model predictions of [9].

Much effort has been devoted in recent years to resolving the puzzle raised by experiments [7–11]. Reference [12] suggested using ultrashort pulses (80 fs) and a heavy molecule, freezing the nuclei during the laser pulse. It was subsequently demonstrated [10], however, that even for I_2 the fragment kinetic energies are essentially independent of the pulse duration in a wide range (~ 80 fs–10 ps), showing that even in very short pulses the molecule tended to ionize around the same critical distance R_{cr} larger than the initial equilibrium value: $R_{cr} > R_{eq}$.

Reference [10] suggested that, owing to collective electron motion in intense laser fields, even highly charged ions (e.g., Cl_2^{8+}), were stabilized against dissociation at some R_{cr} . It was pointed out [10], however, that this interpretation is hard to reconcile with the independence of the “constant energy ratio” on the intensity.

We suggest that the long-standing experimental puzzle can be accommodated within a more general molecular ionization model described below. We show that intense field molecular ionization differs *qualitatively* from atomic ionization: It depends sensitively on the molecular configuration and hence provides a probe of molecular structure and motions. Although we concentrate on diatomic molecules, our qualitative conclusions extend to larger systems (see [13]). The sensitivity of the ionization rate to the internuclear separations provides an additional mechanism for time-resolving dissociative dynamics using intense laser fields. As will become clear from the discussion below, it is also important for cluster ionization [14], plasma formation [15], charge transfer [16], and dielectric breakdown in femtosecond experiments [17].

In this paper we give a detailed description of our “explosive ionization” model, which was briefly described in our previous papers [18]. In particular, we discuss in detail various tunneling ionization mechanisms proposed in [18] and confirm them with numerical results. We study numerically the possibility of laser-induced suppression of the dissociation proposed in [10]. We also develop a quantitative analytical model of enhanced ionization. The model is based on the theory of laser-enhanced electron localization [19–22] and tunneling ionization [23]. Unlike the analytical model described in our previous paper, it is applicable at all internuclear distances R .

One feature of our model, which has been recognized earlier in [9] and recently extended in [24] is the role played by the inner barrier, between the two nuclei, in molecular ionization. The key additional features of our model are the role of laser-enhanced electron localization and of resonant tunneling (see Sec. IV), as well as the quantitative analytical and numerical description. More recent three-dimensional (3D) numerical simulations of H_2^+ [25] confirm our predictions.

The paper is organized as follows: Sec. II describes our numerical model, and Sec. III describes the results of nu-

merical simulations. In Sec. III A we investigate the possibility of field-induced stabilization against dissociation. In Sec. III B we show that ionization is strongly peaked in a certain window of internuclear distances, for several successive charge states of a diatomic ion, with the peak ionization rate for highly charged states either above or comparable to that for a singly charged state near equilibrium. In Sec. IV we give the qualitative interpretation of our results, showing that the effect of enhanced ionization is a consequence of another strong-field effect: nonadiabatic electron localization in the molecular ion, which has no analogy in the atomic case. We then develop an analytical model, which is based on our interpretation of the numerical results and is applicable at both large and small internuclear separations. Based on our results, in the concluding section we suggest a scenario of multiple dissociative ionization of diatomic molecules, which qualitatively explains the experimental puzzle raised in [10]. We discuss implications of our ionization mechanism to other physical problems, such as cluster ionization and optical breakdown in ultrashort pulses.

II. MODEL

The quantitative description of strong-field ionization of a diatomic ion is performed both numerically and analytically. The numerical approach is based on solving the time-dependent Schrödinger equation for a model diatomic ion with electron motion confined to one dimension. The analytical model described in detail in Sec. IV is based on modification of a well-known 3D atomic intense field-ionization theory [23] and the Landau-Zener theory of nonadiabatic transitions. The numerical model is limited to odd-charged ionic states of the molecule, while the analytical model is applicable to both even and odd charge states.

Numerically, we consider a generic diatomic ion A_2^{n+} aligned along the electric-field vector of the linearly polarized light $E(t) = Ef(t)\cos\omega t$ [$f(t)$ is the envelope]. The ionization dynamics is studied in a single active electron approximation, for a one-dimensional potential

$$V(x|R) = -\frac{Q}{\sqrt{(x-R/2)^2 + a^2}} - \frac{Q}{\sqrt{(x+R/2)^2 + a^2}}. \quad (1)$$

The Coulomb repulsion between the nuclei is $V_c(R) = Q^2/\sqrt{R^2 + a^2}$. (Atomic units are used throughout the paper.)

The time-dependent Hamiltonian for the electron motion in our model system is

$$H(t) = -\frac{1}{2}\nabla^2 + V(x|R) - xE(t). \quad (2)$$

Molecular alignment assumed in our model is believed to be typical in strong-field molecular ionization experiments [26,27]. In addition, typically only laser-aligned ionic fragments are detected [10–12]. Confining the electron motion to one dimension proved to capture the essential features in studying intense-field atomic ionization [28], and we expect it to be particularly reliable in the aligned diatomic case. In Eq. (1) Q is the nuclear charge and a is a smoothing parameter, routinely employed in strong-field atomic ionization theories [28].

The time-dependent Schrödinger equation for an electron motion is solved at each value of R by exact wave-packet propagation, using the split-operator fast-Fourier-transform method. The initial state is taken to be the ground eigenstate of the field-free molecular ion. We assume slow turn on of the electric field, $f(t) = 1 - \exp(-t/\tau)$ in Eq. (2) with τ sufficiently large with respect to both field period and the period of electron motion. The ionization rate is computed by following the time decay of the norm

$$\gamma(R) = - \left\langle \frac{d}{dt} \ln \left| \Psi(x, t|R) \right|^2 \right\rangle, \quad (3)$$

where the outer bracket denotes the time average over the field period. Particular care is taken to ensure that the decay is single exponential by turning the laser field smoothly enough and by propagating the wave packet to sufficiently long times.

A complementary picture of the ionization dynamics is obtained by calculating the total ionization probability following a short pulse, with pulse envelope $Ef(t) = E \sin(\pi t/T)$, where T is the pulse duration. The two measures, the ionization rate and the total ionization probability after a short pulse, correspond to two limiting situations, the former being independent of the experimental details and the latter being independent of a specific decay law.

The time-dependent electronic wave function $\Psi(x, t|R)$ is used also to obtain the Born-Oppenheimer quasienergy potential surfaces of a *dressed molecule*. This is done for the particular case of A_2^{3+} [i.e., $Q=2$ in Eq. (1)]. Analysis of dressed potential surfaces for this relatively low charge state is given to explore the hypothesis formulated in Ref. [10], namely, that intense laser fields induce electron motion which can suppress dissociation of highly charged diatomic ions.

According to the Floquet theorem, for slow ionization the time dependence of $\Psi(x, t|R)$ is given by the following formula:

$$\Psi(x, t|R) = \sum_n e^{-i\epsilon_n(R)t} \Phi_n(x, t|R), \quad (4)$$

where $\Phi_n(x, t|R)$ are periodic functions of time (quasienergy eigenstates of a time-dependent Hamiltonian) and $\epsilon_n(R)$ are R -dependent (complex) quasienergies which represent the Born-Oppenheimer potential surfaces of a dressed diatomic molecule. These surfaces can easily be found, e.g., by Fourier-transforming $\Psi(x, t|R)$ at some x . The quasienergy spectrum $\epsilon_n(R)$ thus obtained is, of course, independent of x . [Nevertheless, the Fourier transformation of $\Psi(x, t|R)$ should be done at several values of x , since some quasienergy wave functions $\Phi_n(x, t|R)$ can accidentally be small at a given value of x .]

The number of dressed potential surfaces obtained this way depends on the initial conditions and the pulse turn-on. Very slow turn-on leads to a predominant population of only one (ground) dressed potential surface, while a fast turn-on gives a richer spectrum. In our calculations of the dressed potential surfaces for A_2^{3+} we used various pulse shapes as well as various initial conditions.

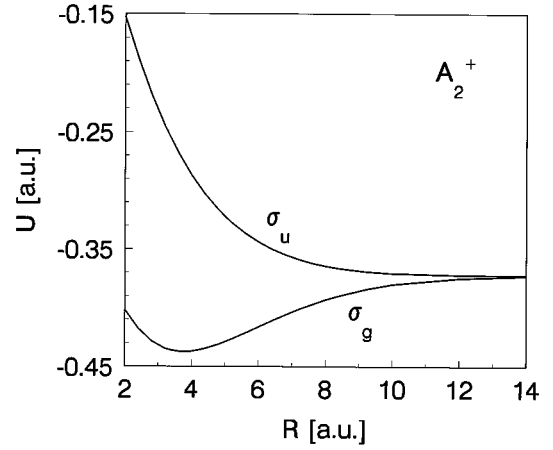


FIG. 1. Field-free potential surfaces of A_2^+ .

III. RESULTS

A. Potential surfaces of a dressed molecule

Before discussing the potential surfaces and strong field dynamics of a field-dressed molecule, we consider our simple one-dimensional model in the field-free case, with the sole purpose of illustrating the structure of field-free potential surfaces. The one-dimensional approximation is well justified in intense linearly polarized fields, where the electron motion is predominantly one dimensional.

Figure 1 shows the Born-Oppenheimer potential surfaces for a model one-dimensional A_2^+ molecular ion [$Q=1$ in Eq. (1)]. Changing the smoothing parameter a in Eq. (1) we can vary the equilibrium distance, ionization potential, and dissociation energy of the model molecule. Although this work is intended to explore a general effect, rather than to model a specific experiment, in order to make the discussion concrete we adjust the parameters of Eq. (1) to correspond roughly to the intensities, wavelengths, and molecular systems probed in experiments (see, e.g., [10–12]). In our calculations we always use $a=2$ and vary Q approximating the ionization potential (and equilibrium distance for a singly charged ion) of diatomic ions such as I_2^{n+} ($n=2Q-1$). Our conclusions are sensitive to neither the value of a nor the precise choice of the field parameters, discussed below.

We next examine the possibility of field-induced stabilization of otherwise unstable molecular ions [10]. Specifically, we consider a triply charged model molecular ion A_2^{3+} . This case corresponds to $Q=2$ in the potential Eq. (1). In the absence of a laser field all potential surfaces of this ion are unstable. The question is whether at least one of them may become stable when the molecule is dressed by the laser field.

Classically, the way to stabilize this system is to force the electron to spend most of its time halfway between the two positively charged nuclei, where a single negative charge can compensate for the Coulomb repulsion between the nuclei. Quantum mechanically, it means that the electron wave function should be compressed by the laser field to a narrow wave packet around $x=0$; the field-free wave function is too broad and does not have enough degree of localization near $x=0$.

Such effects may indeed occur in very high-frequency fields, $\omega \gg I_p(R)$ [29]. At high frequencies we can use the Kramers-Henneberger transformation to change to a reference frame oscillating with the free electron, with amplitude $\alpha = E/\omega^2$. In the new reference frame the interaction with the field is transformed to a time-dependent oscillating field $V(x + \alpha \cos \omega t | R)$, with $V(x | R)$ given by Eq. (1).

We can expand $V(x + \alpha \cos \omega t | R)$ in the Fourier series and, if the laser frequency is large enough, keep only the dominant zero-order term, $V_0(x, \alpha | R) = \int_0^{2\pi} dy V[x + \alpha \cos(y) | R] / (2\pi)$. Each well of the field-free double-well potential (1) is now split into two, with distance 2α between them, similar to the well-known atomic case (see, e.g., the collection of papers in [30]). If the internuclear distance R is equal to 2α , two of these four wells merge into one, creating a triple-well potential with a deeper well exactly in the middle. As a result, the unstable molecule can be stabilized by the field near $R_{eq} \approx 2\alpha$.

Although a similar mechanism is very unlikely to occur for low-frequency fields, we studied the Floquet potential surfaces of A_2^{3+} for various field strengths ($E = 0.02 - 0.06$ a.u., i.e., $I = 1.3 \times 10^{13} - 1.3 \times 10^{14}$ W/cm²) and frequencies ($\omega = 0.03 - 0.06$ a.u.), which are the typical experimental parameters. We were unable to find any values of E, ω in this range for which at least one potential surface of the dressed model molecule is bound. In fact, we found an opposite effect: intense low-frequency fields tend to suppress the deviations of the repulsive potential surfaces from the simple Coulomb law. This is exactly what one would expect as a result of field-enhanced electron localization (see [18] and Sec. IV). As a result, at intensities close to $I = 10^{14}$ W/cm² and for frequencies $\omega = 1.0 - 1.6$ eV the nuclear dynamics of the dressed molecule A_2^{3+} is much closer to a simple Coulomb repulsion, than in the field-free case.

Thus our calculations do not support the hypothesis suggested in Ref. [10]. Since our model includes only one electron, we cannot completely rule out the possibility of molecular stabilization due to some collective multielectron dynamics. However, such collective dynamics can only stabilize highly charged states (e.g., Cl_2^{8+}) if the electrons move coherently, as one particle with a high charge, spending most of the time between the nuclei. If that were the case, one would expect a one-electron model to predict at least some degree of stabilization, but our calculations show the opposite effect.

B. Ionization dynamics

We now look at the ionization rates for several charge states of our model molecule, as a function of R . Within the Floquet formalism these are given by the width of the dressed potential surfaces (the widths of the Floquet components in the molecular spectrum at each R).

As described in Sec. II, we performed two complementary calculations. In both cases we started with the ground electronic state of the molecule. To determine ionization rates we turned the laser field on slowly, $Ef(t) = E[1 - \exp(-t/\tau)]$ with $\tau \approx 20$ fs, ensuring that only the Floquet state corresponding to the field-free ground state was populated. To determine ionization probabilities, we used a very short pulse, $Ef(t) = E \sin(\pi t/T)$ with $T = 30$ fs [full width at half

maximum (FWHM) = 15 fs], in which case many Floquet states are populated. Figures 2(a), 2(b), and 2(c) show, respectively, the ionization rates and ionization probabilities, for several charge states of the model molecule.

There are several important features in the results of our calculations (Fig. 2.) First, all charge states show strongly enhanced ionization in the same region of internuclear separations. One can speak of a critical window of internuclear distances around $R = 8 - 11$ a.u., where several successive ionization stages of the model molecule have a very high ionization rate.

Second, the general envelope of the ionization rate is insensitive to the laser frequency in the range we have studied ($0.8 \text{ eV} \leq \omega \leq 1.6 \text{ eV}$), especially at large R , although the superimposed resonance structure is sensitive to ω [Fig. 2(b)].

Third, although the region of R where the ionization rate is maximum shrinks with increasing charge, the peak value of the ionization rate remains amazingly high while the ionization potential varies from about 25–30 eV (A_2^{3+}) to about 60–70 eV (A_2^{7+}). For the triply charged ion, the ionization rate is almost three orders of magnitude greater near its peak than at $R \rightarrow \infty$. For higher charge states the enhancement is even greater. At $I \approx 9 \times 10^{13}$ W/cm² the ionization rate of A_2^{1+} near equilibrium is almost an order of magnitude less than that of A_2^{3+} near the peak. Only a slight increase in intensity to $I \approx 1.3 \times 10^{14}$ W/cm² is required to achieve an ionization rate of A_2^{5+} and A_2^{7+} comparable to that of A_2^{1+} near equilibrium. It would require approximately one order of magnitude greater intensity to achieve the same ionization rate for an atomic ion A^{3+} .

At higher intensities ($I \sim 10^{15}$ W/cm²) the R dependence of the ionization probability for highly charged ions remains qualitatively the same, with a well pronounced peak at $R \approx 8 - 11$ a.u. The width of the peak increases and the contrast with the ionization rate at infinite R decreases, resulting in a curve very similar to that for A_2^{3+} at $I \sim 10^{14}$ W/cm².

IV. QUALITATIVE PHYSICS AND ANALYTICAL THEORY

In this section we present a qualitative interpretation of the results of our numerical calculations and propose an analytical theory applicable for all internuclear distances. Our analytical model is based on the qualitative physical interpretation suggested below. Its agreement with the numerical data confirms the validity of our qualitative picture.

As noted in Sec. III, the general behavior of the R dependence of the ionization rate is almost independent of laser frequency in the range we studied $\omega = 0.8 - 1.6$ eV. In atoms this is typical for tunnel ionization, which is understood in terms of a *quasistatic* picture. In this picture the phase of the oscillating electric field $E \cos \omega t$ is treated as a parameter and the ionization rate is calculated at each phase of the slowly varying electric field. A similar quasistatic approach is used here. However, the double-well nature of the potential for the electron motion in a molecular ion leads to an important difference compared to the atomic case. We will see that the electron motion between the nuclei is the crucial element in the ionization dynamics. Unlike transitions to the continuum, the electron motion between the discrete states of the double-well molecular potential is nonadiabatic. That is,

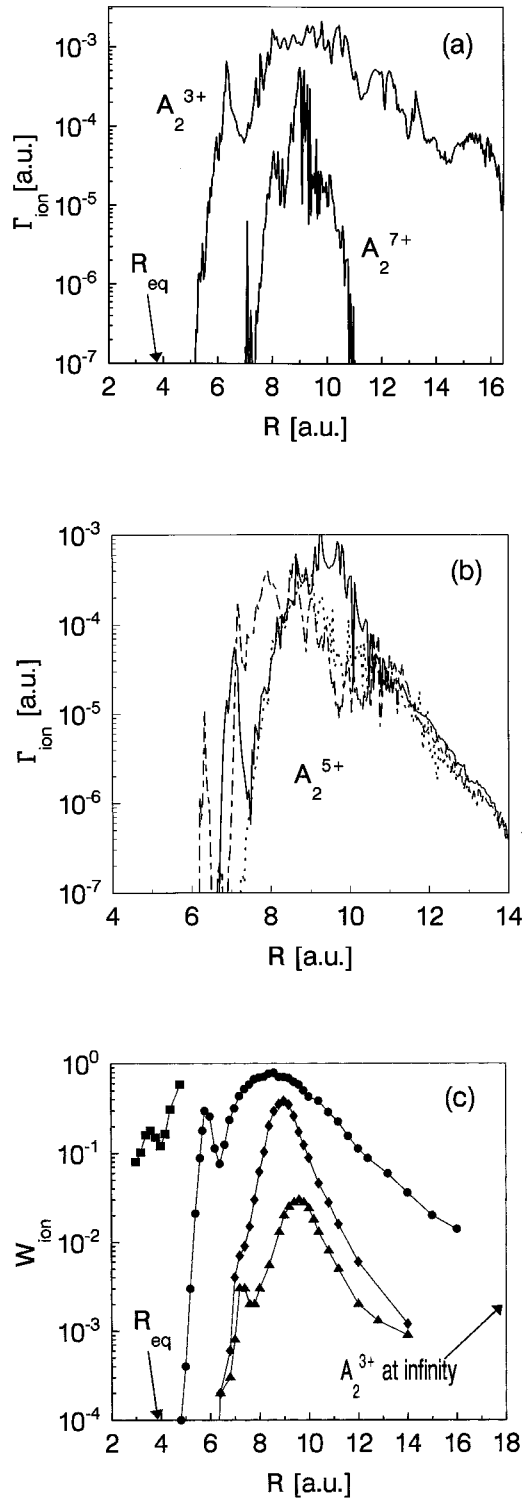


FIG. 2. Ionization of different charge states of a model molecule. (a) Ionization rates of A_2^{3+} and A_2^{7+} at $I=8.75 \times 10^{13}$ W/cm² and $I=1.26 \times 10^{14}$ W/cm², respectively. The laser frequency is $\omega=0.04$ a.u. (b) Ionization rates of A_2^{5+} for three different laser frequencies: $\omega=0.03$ a.u. (dotted line), $\omega=0.04$ a.u. (dashed line), $\omega=0.05$ a.u. (solid line); intensity 1.06×10^{14} W/cm². (c) Ionization probability after the end of the short pulse $I(t)=I \sin^2(\pi t/T)$, $T=30$ fs, for laser frequency $\omega=0.05$ a.u. full squares: A_2^{3+} at $I=8.75 \times 10^{13}$ W/cm²; full circles: A_2^{3+} at $I=8.75 \times 10^{13}$ W/cm²; full triangles: A_2^{5+} at $I=8.75 \times 10^{13}$ W/cm²; full diamonds: A_2^{5+} at $I=1.26 \times 10^{14}$ W/cm².

as the phase of the electric field $E \cos \omega t$ changes during the laser cycle, the electron does not necessarily stay in the state which adiabatically follows the evolution of the electric-field phase. Nevertheless, in the limit of strong interaction, the adiabatic basis is very convenient and, once nonadiabatic transitions are included in the formalism, allows one to describe the electron dynamics in a very physical way. (The convenience of such an approach in the intense-field limit was realized some fifteen years ago; see [19,20]. For example, Ref. [20] shows in detail how Floquet states and multiphoton resonances, which refer to dynamics during many laser cycles, can be rigorously and conveniently described using quasistatic (adiabatic) basis, which follows the system dynamics within each laser cycle.)

A. Low-charge states

Figure 3 shows the Coulomb potential experienced by a valence electron of a diatomic ion $A_2^{(2Q-1)+}$ ($Q=1,2,\dots$) in the absence of a field [Fig. 3(a)] and in the presence of a constant electric field [Fig. 3(b)]. At small internuclear distances (dashed curves) the energy of the local maximum is much lower than the energy of the ground electronic state and ionization is similar to that of an atomic ion, the only difference being the polarizability of molecular ions. At large internuclear distances (dot-dashed curves) the inner barrier between the two wells is broad and ionization is again atomic-like.

By contrast, at intermediate internuclear separations (solid curves), the double-well nature of the molecular potential leads to a *qualitative* difference in the ionization dynamics compared with the atomic case. Figure 3(c) suggests that in this region ionization of diatomic ions would be dramatically enhanced compared to atomic ionization since the electron can tunnel through the narrow *internal* barrier directly to the continuum. A similar figure to Fig. 3(c) was included in an early molecular ionization paper [9]. However, Thomas-Fermi calculations of molecular ionization [31], which followed Ref. [9], were performed in the *adiabatic* limit and showed only very modest enhancement in the ionization rate with internuclear separation. In the adiabatic approximation the electronic wave function adjusts as the potential changes during the laser cycle, fully localizing in the lower well in Fig. 3(c), making ionization much more difficult.

Nonadiabatic localization of (a part of) the electronic wave function in the rising well of the potential is a crucial element of our theory. If, during the laser half-cycle, substantial population is left in the rising well of the double-well potential, a new ionization mechanism is introduced—tunneling of this population to the *continuum* through the internal barrier [Fig. 3(c)], near the peak of the instantaneous electric field $E \sin \omega t$.

Electron localization in one of the wells of the double-well potential is known to occur in double-well quantum structures [21]. Note that complete electron localization is not required in our case. We only require that during the laser *half cycle* there is a substantial probability for the electron to stay in the rising well, rather than to make an adiabatic transition to the descending well. In sufficiently strong laser fields (or for sufficiently large R), when $RE \gg \omega_{ug}(R)$, where $\omega_{ug}(R)$ is the splitting between the ground (gerade) state and its ungerade partner, this transition is only possible

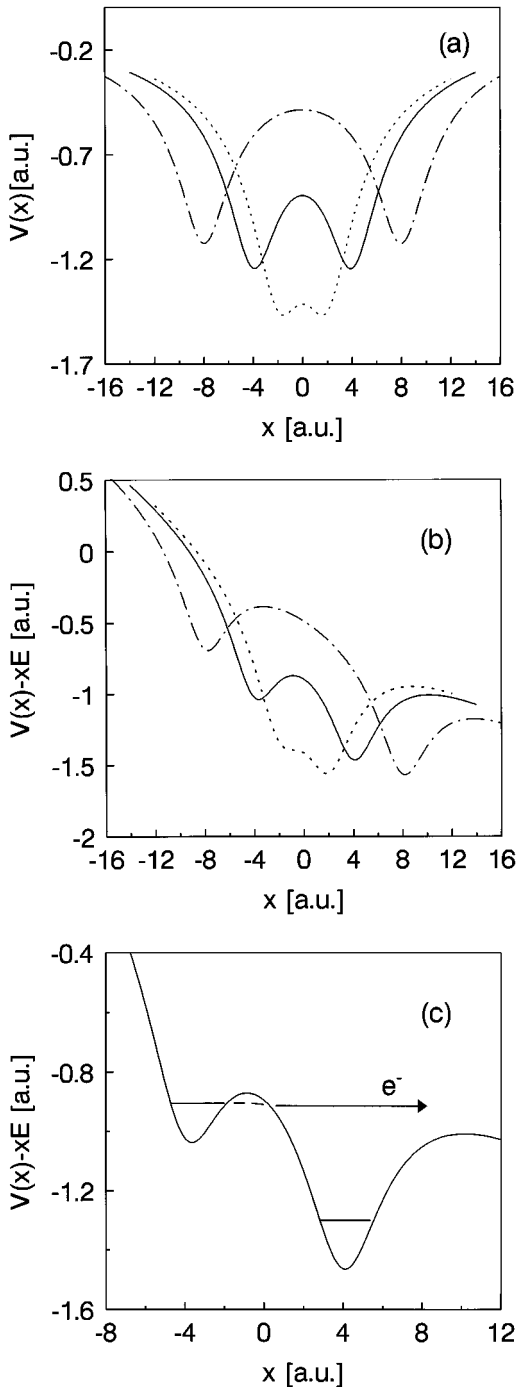


FIG. 3. Pictorial scheme of the electronic potential at several internuclear separations: dotted line $R=4$ a.u., solid line $R=8$ a.u., dot-dashed line $R=16$ a.u. (a) without electric field, (b) with electric field, (c) tunneling ionization through internal barrier.

during a short fraction of the laser half cycle near the *zero* of the instantaneous field, when $RE \sin \omega t \leq \omega_{ug}(R)$. Therefore, tunneling to the continuum (bound-free transition), which occurs near the *peak* of the instantaneous field, is *separated in time* from possible adiabatic transition between the two wells (bound-bound resonance tunneling), which occurs near the *zero* of the instantaneous field.

Quantitatively, the effect of electron localization and trapping of population in the rising well can be described by solving the Schrödinger equation for a two-level system of

ground gerade $|g\rangle$ and excited ungerade $|u\rangle$ states. If the electron wave function is a symmetric superposition of these two states $|\phi(t=0)\rangle = (|u\rangle + |g\rangle)/\sqrt{2}$, it is localized near the left nucleus. Let free, in a time $T_{ug} = \pi/\omega_{ug}$ it will evolve into $|\phi(t=\pi/\omega_{ug})\rangle = (|u\rangle - |g\rangle)/\sqrt{2}$, a state localized near the right nucleus. The time $T_{ug} = \pi/\omega_{ug}$ is the time of electron motion between the nuclei. In the presence of a strong laser field $RE \gg \omega_{ug}(R)$ the field-free splitting $\omega_{ug}(R)$ is changed to [22]

$$\omega_{ug}(R, E) = \omega_{ug}(R) J_0(RE/\omega). \quad (5)$$

Equation (5) is applicable when $\omega > \omega_{ug}(R)$ or, for small laser frequencies $\omega < \omega_{ug}(R)$, when $RE\omega > \omega_{ug}^2(R)$. As one can see from Eq. (5), in strong fields, when

$$RE \gg \omega_{ug}(R), \quad \omega_{gu}^2(R)/RE\omega < 1 \quad (6)$$

the frequency of electron motion between the nuclei decreases [the time $T_{ug}(R, E) = \pi/\omega_{ug}(R, E)$ increases]. Complete suppression of electron motion between the nuclei occurs when the Bessel function in Eq. (5) is equal to zero. In general, however, it is required that the transition frequency in the field $\omega_{ug}(R, E) = \omega_{ug}(R) J_0(RE/\omega)$ be smaller than the laser frequency ω . When this condition is fulfilled, trapping of the electron in the rising well of the potential is efficient and tunneling through the inner barrier directly to the continuum [Fig. 3(c)] may occur. At large R , when $\omega > \omega_{ug}(R)$, the condition $\omega > \omega_{ug}(R, E)$ is satisfied for all values of E . At intermediate R , when $\omega < \omega_{ug}(R)$, the requirement $\omega > \omega_{ug}(R, E)$ is met when the conditions Eq. (6) are satisfied. It is easy to verify that, for our model molecule, the condition $\omega > \omega_{ug}(R, E)$ is satisfied near the peak of the ionization rate curve ($R \sim 8-10$ a.u.), for laser frequencies and intensities used in the calculations. For example, in the case of A_2^{3+} , for $E=0.05$ a.u. ($I=8.75 \times 10^{13}$ W/cm²), $\omega=0.05$ a.u., we obtain $\omega_{gu}(R)/\omega=0.056$ for $R=8$ a.u.

B. High-charge states

The ionization mechanism becomes more complex as one moves to higher charge states (e.g., A_2^{5+} , A_2^{7+}), keeping the laser intensity constant. For large Q in Eq. (1) the ground state in each of the wells of the double-well potential is very deeply bound. At the intensities shown in Fig. 2(b) the external barrier is not suppressed to below the ground state of the raised well [Fig. 4(a)] until very large R . However, for large Q each well supports more than one localized state even at modest R . These high-lying excited states [state |4⟩ in Figs. 4(a), 4(b)] have sufficient energy to tunnel to the continuum at the intensities considered.

The excitation mechanism of these states can be qualitatively understood as resonant tunneling [see Figs. 4(a) and 4(b)], and can be described within the Landau-Zener formalism. This excitation mechanism is known to occur in quantum well devices [32]. During the laser half cycle the localized ground state of the rising well [state |2⟩ in the left well in Fig. 4(a)] passes through resonance with excited states of the descending well [state |3⟩ in the right well in Fig. 4(a)]. This leads to an avoided crossing in Fig. 4(b). After the avoided crossing, a fraction of the population is transferred to the excited state of the descending well via *adiabatic*

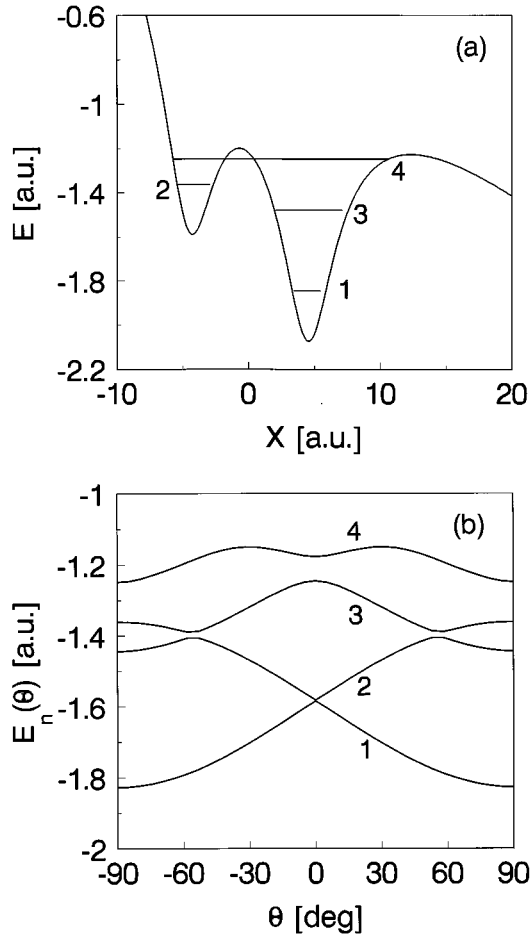


FIG. 4. Pictorial scheme of resonant tunneling ionization mechanism for $R=9$ a.u. and A_2^{5+} at $I=1.06 \times 10^{14}$ W/cm². (a) Double-well potential at the peak of the electric field with adiabatic levels; (b) adiabatic levels vs the phase $\phi = \omega t$ of the electric field $E \sin \omega t$. Avoided crossings are the points of nonadiabatic or adiabatic (resonant tunneling) transitions.

Landau-Zener-type transition. This transition corresponds to tunneling through the internal barrier during the resonance between states $|2\rangle$ and $|3\rangle$. On the way back, when the right well rises and the left well descends, a *diabatic* Landau-Zener-type transition [Fig. 4(b)] is needed to keep the population in the excited state of the rising well. Thus excitation results from resonant tunneling and requires one adiabatic and one diabatic transition. The peak position of the ionization curve is determined by the competition between excitation and tunneling to the continuum, as well as by an optimum in excitation.

We note that similar physics is found in microwave excitation and ionization of alkaline Rydberg atoms [33,34]. Recent experiments on excitation of alkaline Rydberg atoms with “microwave” half-cycle pulses [34] gave a convincing demonstration of the same physical mechanism of sequential diabatic and adiabatic Landau-Zener-type transitions. Increasing amplitude in the half-cycle pulse produces the usual Stark manifold of Rydberg $|nl\rangle$ states with a negligible quantum defect ($l > 2$). At some value E_c of the electric field this manifold mixes with the initially populated lower-lying state $|n_0 l_0\rangle$ with small l_0 and large quantum defect. As the field E passes the value E_c , population can be adiabatically

transferred from the state $|n_0 l_0\rangle$ to the Stark states. As the field in the half-cycle pulse decreases, E_c is passed again, and this time diabatic transition is needed to keep the population in the states $|nl\rangle$ [34].

Returning to molecules, if the laser intensity is increased to $I \sim 10^{15}$ W/cm², then the resonant tunneling ionization mechanism is replaced by a simpler one-step tunneling through the inner barrier at higher intensities. The ionization probability increases and its R dependence becomes very similar to that for A_2^{3+} at $I \approx 10^{14}$ W/cm².

C. Analytical model

We now describe a 3D analytical model valid in the low-frequency–high-intensity limit. The model is applicable at all internuclear distances. It is based on the qualitative interpretation of our numerical results and consists of two steps. First, we find the population of ground and excited adiabatic states near the peak of the instantaneous electric field. For odd-charge states this is done in a two-level approximation. That is, we only consider the ground (gerade) state of the double-well potential and its charge-resonant (ungerade) partner. For even-charge states at small and intermediate R the two levels are the ground state and its charge-transfer partner of the opposite symmetry. At large R both symmetric $|s\rangle$ and asymmetric $|a\rangle$ charge-transfer states have to be included. However, at this stage the dynamics can again be reduced to a two-level model by using sum and difference states $|a\rangle \pm |s\rangle$, which are decoupled from each other, degenerate, and have equal couplings to the ground state. Second, we calculate the probability of tunnel ionization from both states near the peak of the field. This approach is valid because, as explained above, nonadiabatic transition between the adiabatic states and tunneling to the continuum occur at different parts of the laser half-cycle: transition to the continuum occurs near the peaks of the instantaneous field, while transition between the adiabatic states occur near the crests.

Below we will concentrate on the simpler case of odd-charge ionic states. The results at large R can be extended to even-charge states without any modification.

Ionization from the upper state. We begin the description of the model with its second step—tunneling ionization from the excited adiabatic state near the peak of the instantaneous field.

(1) At large internuclear distances the external barrier is irrelevant near the peak of the instantaneous electric field: ionization can be envisioned as tunneling through the internal barrier, suppressed by the *combined* electric fields of the laser and the adjacent ion, $\mathbf{E}_{\text{tot}} = \mathbf{E} \sin \omega t + \mathbf{E}_{\text{ion}}$. (Note that for the *upper* adiabatic state both fields are acting in the same direction during the whole laser cycle, yielding $E_{\text{tot}} = E|\sin \omega t| + |\mathbf{E}_{\text{ion}}|$.) This hints at modifying the standard 3D atomic tunneling ionization theory (ADK) [23] by replacing the laser field $E \sin \omega t$ with E_{tot} . The main difficulty of this approximation is that the field of the adjacent ion is not constant, but depends on the distance from the ion. However, tunneling is efficient only when the barrier is sufficiently low and thin, so that the field of the adjacent ion is approximately constant across the barrier. We therefore find the maximum of the potential barrier for the exact potential $V(x|R)$

$-xE \sin \omega t$ and then replace the inhomogeneous field of the adjacent ion by the homogeneous field calculated at the maximum of the potential barrier: $E_{\text{tot}} = E|\sin \omega t| + Q_2/(R-R_0)^2$, where Q_2 is the charge of the adjacent nucleus and $R_0 = R_0(E \sin \omega t, Q_1, Q_2)$ accounts for the offset of the barrier maximum from the nucleus with charge Q_1 , at which the upper adiabatic state is localized.

(2) At small internuclear distances the external barrier becomes important. We therefore have to include the corresponding tunneling probability. Now the upper-state wave function is distributed along the whole double-well potential and it is natural to use the standard ADK theory [23] modified to include the Stark shift of the upper state and the R -dependent field-free ionization potential of the upper state $I_{p,2}(R)$.

In general, one has to include tunneling through both barriers, although for most internuclear distances one of the two barriers is suppressed below the upper adiabatic state and the corresponding transmission coefficient is equal to one. An approximate formula which describes this general situation is

$$w_{\text{upper}}(t) = w_1(t)w_2(t)/[w_1(t) + w_2(t)], \quad (7)$$

where $w_1(t)$ is the tunneling rate through the inner barrier and $w_2(t)$ is the tunneling rate through the external barrier. When one of the two rates is much smaller than the other, this smaller rate determines the rate of the whole process. According to the above discussion, the rate $w_1(t)$ can be written as

$$w_1(t) = w_{\text{ADK}}[I_p(R \rightarrow \infty); E_{\text{tot}}; Q_1], \quad (8)$$

while the rate $w_2(t)$ is

$$w_2(t) = w_{\text{ADK}}[I_{p,2}(R) - \Delta(E \sin \omega t, R); E \sin \omega t; Q_1 + Q_2]. \quad (9)$$

Here $I_{p,2}(R)$ is the field-free ionization potential of the excited state, $\Delta(E \sin \omega t, R)$ is the Stark shift of the excited state in the adiabatic approximation. $Q_1 + Q_2$ is the total charge of the two nuclei, and $w_{\text{ADK}}(I_p; E; Q)$ denotes the standard ADK ionization rate [23] for the ionization potential I_p , electric field E , and nuclear charge Q .

We now have to include the relative population of the upper adiabatic state. For slow turn-on of the laser field the system initially prepared in the ground state goes into the ground Floquet state $\Psi_g^{(F)}$. To find the decay rate of the system via the upper adiabatic state, the wave function of the ground Floquet state has to be projected onto the upper adiabatic state $\Psi_{\text{upper}}^{(\text{ad})}$. Averaged over resonances, in a two-level approximation this yields the following result [19]:

$$|\langle \Psi_g^{(F)} | \Psi_{\text{upper}}^{(\text{ad})} \rangle|^2 = 0.5 \left(1 - \frac{\sqrt{1-Z}}{\sqrt{1+Z}} \right), \quad (10)$$

where

$$Z = \exp \left(- \frac{2\omega_{12}}{\omega} \frac{D[1/(1+q^2)]}{\sqrt{1+q^2}} \right) \quad (11)$$

and $q = 2Ed_{12}(R)/\omega_{12}(R)$, d_{12} being the transition matrix element in the two-level system. For odd-charge states of the

molecular ion $d_{12} \approx R/2$ and $q \approx ER/\omega_{12}(R)$. In Eq. (11) $D(x)$ is the elliptic integral of the third kind

$$D(x) = \int_0^{\pi/2} \frac{\sin^2 \theta}{\sqrt{1-x \sin^2 \theta}} d\theta. \quad (12)$$

We note that the projection of the Floquet state onto the upper adiabatic state is, of course, normalized to the total population left in the two-level system. That is, it gives a *fraction* of the total population, which is residing in the upper adiabatic state. Such normalization is required since the decay rate is also always normalized to the total population of the system.

In the limit $q \gg 1$, that is, $RE \gg \omega_{12}(R)$, the expression Eq. (10) becomes

$$|\langle \Psi_g^{(F)} | \Psi_{\text{upper}}^{(\text{ad})} \rangle|^2 = 0.5 \exp(-\pi\omega_{12}^2(R)/2RE\omega). \quad (13)$$

In the limit $\omega_{12}^2(R)/2RE\omega \ll 1$ this expression has to be corrected to include coherent effects in the destruction of tunneling, caused by interference of transitions during successive laser half cycles [20]. Taking into account that in this limit $\omega_{12}(R, E) = \omega_{12}(R) \sqrt{2\omega/\pi RE \sin(RE/\omega + \pi/4)}$, the correct expression is $|\langle \Psi_g^{(F)} | \Psi_{\text{upper}}^{(\text{ad})} \rangle|^2 = 0.5 \exp\{-\pi\omega_{12}^2(R) \sin^2(RE/\omega + \pi/4)/RE\omega\}$.

Hence the contribution of the upper adiabatic state to the ionization rate of the diatomic ion prepared in its ground Floquet state is

$$\Gamma_u(t) = 0.5 \left(1 - \frac{\sqrt{1-Z}}{\sqrt{1+Z}} \right) \frac{w_1(t)w_2(t)}{w_1(t) + w_2(t)}, \quad (14)$$

where the rates $w_1(t)$ and $w_2(t)$ are given by Eqs. (8),(9).

Ionization from the lower state. The ionization rate from the lower adiabatic state is again obtained by using the ADK theory. Tunneling from this state contributes to the total ionization rate in two cases. First, its contribution is significant at very small internuclear distances, where no electron localization takes place and population of the upper state is negligible. Second, its contribution is significant at very large internuclear distances, where the internal and the external barriers are almost identical and the enhancement of ionization due to the field of adjacent ion is negligible. At intermediate distances shown in Figs. 2 and 5 the contribution of the lower state is negligible.

As shown in [35], at small internuclear distances the ionization rate is obtained by minor modifications of the standard ADK tunneling theory: using R -dependent field-free ionization potential and including molecular polarizability. At large internuclear distances the ionization rate is given by the ADK theory modified similar to Eq. (8), but now the total field E_{tot} is given by the *difference* between the laser field and that of the adjacent ion: $E_{\text{tot}} = E|\sin \omega t| - E_{\text{ion}}$. The fraction of the population residing in the lower adiabatic state, normalized to the total population left in the system, is $|\langle \Psi_g^{(F)} | \Psi_{\text{lower}}^{(\text{ad})} \rangle|^2 = 1 - |\langle \Psi_g^{(F)} | \Psi_{\text{upper}}^{(\text{ad})} \rangle|^2$.

The total ionization probability is

$$W_{\text{ion}} = 1 - \exp \left(- \int [\Gamma_u(t) + \Gamma_l(t)] dt \right). \quad (15)$$

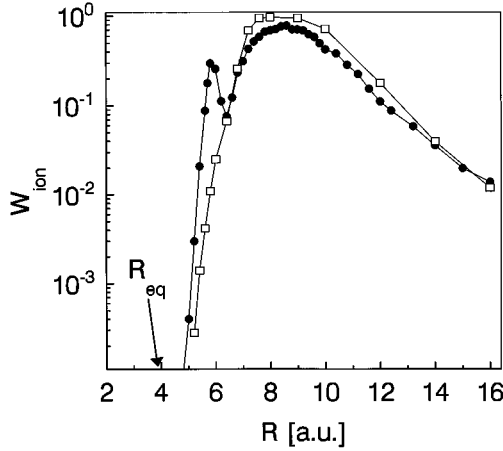


FIG. 5. Comparison of numerical and analytical calculations of ionization probability for A_2^{3+} at the end of short pulse $I(t) = I \sin^2(\pi t/T)$, $T = 30$ fs, for laser frequency $\omega = 0.05$ a.u. Full circles—1D numerical simulations at $I = 8.75 \times 10^{13}$ W/cm², open squares—3D analytical results at $I = 1.35 \times 10^{14}$ W/cm². Intensity in analytical calculations is chosen to match ionization rate at $R = 16$ a.u.

We have applied this analytical model to our model triply charged molecular ion A_2^{3+} (Fig. 5). The open squares and the full circles in Fig. 5 compare the analytical and the numerical ionization probabilities for A_2^{3+} after the end of the laser pulse $Ef(t) = E \sin(\pi t/T) \sin \omega t$. The pulse parameters are the same as in Fig. 2(c). Since tunneling in 3D is less efficient than in 1D, we had to increase intensity in the analytical calculations to approximately match numerical calculations at large $R = 14$ – 16 a.u. The very simple 3D quasistatic analytical model agrees quite well with the exact solution of the 1D time-dependent Schrödinger equation. In the critical region of R the ionization rate is overestimated by the analytical formula. The reason is the extreme sensitivity of the Γ_{ion} to laser intensity in the critical region and higher intensity used in the analytical calculations. Small deviations in the ionization probability at small R result from a breakdown of the tunneling approximation.

Agreement between the analytical 3D model and the numerical 1D calculation confirms our qualitative interpretation of the results. Most important is that for sufficiently large internuclear distances, when the electron motion between the nuclei on the time scale of a laser cycle is negligible, we can look at ionization of a molecular ion as at the ionization of an atomic ion in the combined electric field of the laser and the adjacent ion. This shows that at sufficiently large R our analytical theory is not restricted to odd-charged molecular ions, but can also be used to describe ionization of even-charged ions A_2^{2n+} . Hence our general conclusions can be immediately extended to even-charged molecular ions.

We note that for H_2^+ , the characteristic R dependence of the ionization rate is implicit in three values ($R = 7$ a.u., 10 a.u., and ∞) of the rate obtained by 3D numerical simulations [36].

V. CONCLUSION

Our results suggest that the following scenario takes place in long-pulse dissociative molecular ionization: First, several

electrons are stripped until the first repulsive charge state (A_2^{2+} or A_2^{3+}) is reached. The molecule starts to dissociate and enters a critical region $R \approx R_{\text{cr}}$, where the ionization rate is strongly peaked for several successive ionization stages. A simple estimate assuming Coulomb repulsion shows that even as heavy a molecule as I_2^{3+} starting to dissociate with zero initial kinetic energy at $R_{\text{eq}} \approx 5$ a.u. will reach the critical region ($R \approx 9$ a.u.) in about 110 fs. As seen, e.g., in Fig. 2(c), the intensity needed to reach the repulsive state A_2^{2+} near equilibrium is sufficient to rapidly ionize several more electrons in the critical region, producing a series of highly charged states. The series is terminated at a state for which the time required for the nuclei to pass the critical region is too short to permit further ionization. Thus, the fragments from all charge states of the molecule have kinetic energies that correspond to Coulomb repulsion at approximately the same internuclear distance R_{cr} . These energies constitute a constant fraction $R_{\text{eq}}/R_{\text{cr}}$ of the Coulomb energy at the equilibrium distance, independent of the charge state and pulse duration. This gives a qualitative answer to the experimental puzzle discussed in Ref. [10].

One can roughly estimate R_{cr} by approximately calculating the distance where the internal barrier penetrates the ground state and the interplay between the two barriers starts to dominate ionization dynamics (see also [18,24]). Using the approximation that the ionization potential of an atomic ion with charge $(Q-1)$ is QI_p , where I_p is the atomic ionization potential, we find that localization occurs at $R_{\text{cr}} \sim 3/I_p$, independent of Q . One obtains $R_{\text{cr}} = 2.87$ (2.34), 3.1 (2.62), 3.1 (2.75), 3.3 (2.8), and 3.9 (3.6) Å for N_2 , O_2 , H_2 , Cl_2 , and I_2 , respectively. The distances shown in brackets are suggested by experimental explosion energies [10,24]. If one includes extra kinetic energy acquired during dissociation between R_{eq} and R_{cr} , the agreement between the rough estimate given above and the experimental data will become even better.

Another important consequence of enhanced ionization is its effect on angular distribution of the multiply charged ionic fragments. The ionization rate in the critical region is highly dependent on the molecular orientation to the field. The molecules aligned parallel to the field are much more likely to reach high ionization stages, and the angular distribution of ionic fragments will be peaked in the direction of the field even if there were no field-induced molecular alignment.

Our results have important implications also for several other fields. An ion in close proximity to an atom, a molecule, or another ion is found in many areas of physics. These include cluster ionization [14], plasma formation [15], and dielectric breakdown [17], to mention but a few. Enhanced ionization which is sensitive to the nuclear coordinates is likely to play a role in all these situations.

Recently, we learned about the experiments on explosive (enhanced) ionization performed by three different groups [37–39]. All three experiments claim to give direct experimental evidence of the effect described in this paper and in [18,24,25]. In particular, in the experiment [37] dissociative ionization of an I_2 molecule up to I_2^{10+} charged state was observed at intensities $I \sim 10^{14}$ W/cm², yielding atomic ions I^{5+} , while ionization of iodine atoms yielded ions I^{2+} only. In the pump-probe experiment [39] the ionization rate of

$I_2^{2+} \rightarrow I + I^{++}$ was measured as a function of the time delay between the pump pulse producing I_2^{++} and the probe pulse ionizing $I_2^{++} \rightarrow I + I^{++}$, with the distinct peak around $R \sim 4\text{--}5 \text{ \AA}$. Similar results are found for other charge states. In the experiment [38] above-threshold dissociation of D_2^+ was observed, yielding a distinct double-peak structure in the kinetic energy of the fragments, with the second (high-energy) peak corresponding to the Coulomb explosion of D_2^{++} at $R \approx 3.6 \text{ \AA}$.

ACKNOWLEDGMENTS

This work benefitted from many inspiring and exciting discussions with D. D. Normand, C. Cornaggia, M. Schmidt, A. Bandrauk, T. Zuo, S. Chelkowski, H. Stapelfeldt, E. Constant, A. Stolow, M. Lewenstein, K. Codling, K. Rzazewski, and D. Villeneuve. M. Ivanov acknowledges financial support from a special NSERC collaborative research grant.

-
- [1] A. L'Huillier *et al.*, Phys. Rev. Lett. **48**, 1814 (1982); Phys. Rev. A **27**, 2503 (1983); J. Phys. B **16**, 1363 (1983).
 - [2] T. S. Luk *et al.*, Phys. Rev. A **32**, 214 (1985).
 - [3] U. Johann *et al.*, Phys. Rev. A **34**, 1084 (1986).
 - [4] M. D. Perry *et al.*, Phys. Rev. A **37**, 747 (1988).
 - [5] K. Boyer and C. K. Rhodes, Phys. Rev. Lett. **54**, 1490 (1985); A. Szöke and C. K. Rhodes, Phys. Rev. Lett. **56**, 720 (1986).
 - [6] P. Lambropoulos, Phys. Rev. Lett. **55**, 2141 (1985).
 - [7] K. Codling *et al.*, J. Phys. B **2**, L525 (1987).
 - [8] L. J. Frajnski *et al.*, Phys. Rev. Lett. **58**, 2424 (1987).
 - [9] K. Codling, L. J. Frajnski, and P. A. Hatherly, J. Phys. B **22**, L321 (1989).
 - [10] M. Schmidt, D. Normand, and C. Cornaggia, Phys. Rev. A **50**, 5037 (1994).
 - [11] K. Codling and L. J. Frajnski, J. Phys. B **26**, 783 (1993).
 - [12] D. Strickland *et al.*, Phys. Rev. Lett. **68**, 2755 (1992).
 - [13] T. Seideman, M. Yu. Ivanov, and P. B. Corkum, Chem. Phys. Lett. **252**, 181 (1996).
 - [14] J. Purnell *et al.*, Chem. Phys. Lett. **229**, 33 (1994); A. McPherson *et al.*, Phys. Rev. Lett. **72**, 1810 (1994).
 - [15] N. H. Burnett and P. B. Corkum, JOSA-B **6**, 1195 (1989); B. E. Lemoff, C. P. J. Barty, and S. E. Harris, Opt. Lett. **19**, 569 (1994).
 - [16] See, e.g., R. Marcus, J. Phys. Chem. **96**, 1753 (1992) and references therein.
 - [17] D. Du *et al.*, Appl. Phys. Lett. **64**, p. 3071 (1994).
 - [18] T. Seideman, M. Yu. Ivanov, and P. B. Corkum, Phys. Rev. Lett. **75**, 2819 (1995).
 - [19] V. P. Krainov, Zh. Eksp. Teor. Fiz. **70**, 1197 (1976) [Sov. Phys. JETP **43**, 622 (1976)]; V. P. Krainov and V. P. Yakovlev, *ibid.* **78**, p. 2204 (1980) [**51**, 1104 (1980)].
 - [20] I. Sh. Averbukh and N. F. Perelman, Zh. Eksp. Teor. Fiz. **88**, 1131 (1985) [Sov. Phys. JETP **61**, 665 (1985)].
 - [21] F. Grossmann *et al.*, Phys. Rev. Lett. **67**, 516 (1991); R. Bavli and H. Metiu, Phys. Rev. Lett. **69**, 1986 (1992); M. Holthaus, Phys. Rev. Lett. **69**, 1596 (1992).
 - [22] J. M. Llorente and J. Plata, Phys. Rev. A **45**, R6958 (1992); M. Ivanov, P. Dietrich, and P. Corkum, Laser Phys. **3**, 375 (1993).
 - [23] M. V. Ammosov, N. B. Delone, and V. P. Krainov, Zh. Eksp. Teor. Fiz. **91**, 2008 (1986) [Sov. Phys. JETP **64**, 1191 (1986)].
 - [24] J. H. Posthumus *et al.*, J. Phys. B **28**, L349 (1995).
 - [25] T. Zuo and A. Bandrauk, Phys. Rev. A **52**, R2511 (1995).
 - [26] D. D. Normand *et al.*, J. Phys. B **25**, L497 (1992); P. A. Hatherly *et al.*, J. Phys. B **23**, L291 (1990).
 - [27] B. Friederich and D. R. Hershbach, Phys. Rev. Lett. **74**, 4623 (1995); T. Seideman, J. Chem. Phys. **103**, 7887 (1995).
 - [28] J. H. Eberly *et al.*, in *Atoms in Intense Laser Fields*, edited by M. Gavrilu (Academic, San Diego, 1992), p. 301.
 - [29] T. Zuo and A. Bandrauk, Phys. Rev. A **51**, R26 (1995) [see also related paper by J. Shertzer, A. Chandler, and M. Gavrilu, Phys. Rev. Lett. **73**, 2039 (1994)].
 - [30] *Atoms in Intense Laser Fields*, edited by M. Gavrilu (Academic, San Diego, 1992).
 - [31] M. Brewczyk and L. Frasiniski, J. Phys. B **24**, L307 (1991).
 - [32] H. C. Liu *et al.*, Phys. Rev. B **48**, 1951 (1993).
 - [33] See, e.g., P. Pillet *et al.*, Phys. Rev. A **30**, 280 (1984); C. R. Mahon *et al.*, *ibid.* **44**, 1859 (1991); M. C. Baruch and T. F. Gallagher, Phys. Rev. Lett. **68**, 3515 (1992); M. Gatzke *et al.*, Phys. Rev. A **50**, 2502 (1994).
 - [34] G. M. Lankhuijzen and L. D. Noordam, Phys. Rev. Lett. **74**, 355 (1995).
 - [35] P. Dietrich and P. B. Corkum, J. Chem. Phys. **97**, 3187 (1992).
 - [36] T. Zuo, S. Chelkowski, and A. Bandrauk, Phys. Rev. A **48**, 3837 (1993).
 - [37] D. Normand and M. Schmidt, Phys. Rev. A **53**, R1958 (1996).
 - [38] F. Ilkov *et al.*, Chem. Phys. Lett. **247**, 1 (1995).
 - [39] H. Stapelfeldt, E. Constant, and P. B. Corkum, Phys. Rev. Lett. **74**, 3780 (1995).